Biochem. Soc. Symp. **46**, 155–181
Printed in Great Britain

Protein Crystals, Membrane Proteins and Membrane Lipids

Recent Advances in the Study of their Static and Dynamic Structures using Nuclear Magnetic Resonance Spectroscopic Techniques

ERIC OLDFIELD, NATHAN JANES, ROBERT KINSEY, AGUSTIN KINTANAR, ROBERT W.K. LEE, T. MICHAEL ROTHGEB, SUSANNE SCHRAMM, ROBERT SKARJUNE, REBECCA SMITH and MING-DAW TSAI

School of Chemical Sciences, University of Illinois at Urbana-Champaign, Urbana, IL 61801, U.S.A.

Introduction

The purpose of this paper is to summarize briefly advances in three different areas which have involved the use of high-field solid-state n.m.r. spectroscopic techniques in our study of the structure of two systems of biological interest. We first discuss a new technique, developed over the last year, which enables us to study in some detail the static structure, and in principle the dynamic structure, of protein crystals. The method basically involves using strong magnetic fields to align microcrystals of specifically-labelled paramagnetic proteins, which permits the recording of (single-crystal) n.m.r. spectra of these systems. We show that it is thereby possible to resolve numerous different sites, and thus to determine the orientations of different groups in these complex macromolecular systems. Second, we discuss recent advances in the study of membrane structure using n.m.r. methods. The first advance involves the observation of ^{2}H n.m.r. spectra of membranes specifically enriched with ^{2}H-labelled amino acids, and examples are given of such spectra from *Acholeplasma laidlawii* and *Halobacterium halobium*. We suggest that it will soon be possible to resolve and perhaps assign most atoms in the membrane protein of *H. halobium*, opening up the possibility of studying energy transduction in some detail. A second aspect of our discussion of membrane proteins focuses on the effects proteins have on lipid acyl chain dynamics, and a model of protein–lipid interaction that involves the slight disordering of hydrocarbon chains, contrary to the popular conception of significant ordering of hydrocarbon chains analogous to that imposed by cholesterol, is discussed. Finally, we note the development of several new techniques involving ^{14}N and ^{17}O n.m.r. which have promise of detailing the static and dynamic structure of membrane lipids, and we also comment on the observation of highly unusual lineshapes in some ^{2}H-labelled membrane systems indicative of rather specialized hydrocarbon chain motions.

Over the past 20 years, there have been an impressive number of studies of the structure of proteins, both in the crystalline solid state (Blundell & Johnson, 1976) and in solution (Dwek, 1973; Wüthrich, 1976). The most direct

information about protein structure most frequently comes from X-ray crystallography of solid samples, while solution structural information has been obtained most directly by n.m.r. spectroscopy. Of the two methods, X-ray diffraction gives direct three-dimensional or spatial structural information, whereas n.m.r. spectroscopy is more suited to determination of the dynamic aspects of protein structure (Gurd & Rothgeb, 1979; Wagner *et al.*, 1976). More recently (Artymiuk *et al.*, 1979; Frauenfelder *et al.*, 1979) X-ray diffraction has also been shown to be very valuable in determining the dynamic structures of protein crystals. In defence of n.m.r. spectroscopy, we have therefore felt it necessary to develop a new n.m.r. technique capable of giving both dynamic and static structural information about proteins in condensed phases, such as crystals and membranes.

While it is doubtful that any method solely capable of confirming the correctness of existing X-ray structures would have any utility, we indicate how our method may be used to determine in protein crystals, too small to be studied by X-ray crystallography, the orientation of various residues, and how it may be used (in principle) to determine in a fairly direct fashion the rates and types of motion, and activation energies for motion, of various residues in protein crystals, which is presumably one of the main reasons for differences between the activities of enzymes and other proteins in solution and in the crystalline solid state (Chance, 1966).

Theoretical Considerations

Quite generally, we can write for a nucleus a Hamiltonian:

$$\mathcal{H} = \mathcal{H}_Z + \mathcal{H}_Q + \mathcal{H}_{DD} + \mathcal{H}_{CSA} + \mathcal{H}_{SC} \qquad (1)$$

where $\mathcal{H}_Z$, $\mathcal{H}_Q$, $\mathcal{H}_{DD}$, $\mathcal{H}_{CSA}$ and $\mathcal{H}_{SC}$ represent the Zeeman, quadrupole, dipole–dipole, chemical shift and scalar coupling interactions, respectively. Now for ^2H ($I = 1$) $\mathcal{H}_{DD}$, $\mathcal{H}_{CSA}$ and $\mathcal{H}_{SC}$ are small and thus we may write:

$$\mathcal{H} = \mathcal{H}_Z + \mathcal{H}_Q \qquad (2)$$

or more explicitly:

$$\mathcal{H} = -\gamma_n \hbar H_0 I_{z'} + \frac{e^2qQ}{4I(2I-1)}(3I_z^2 - I^2) \qquad (3)$$

where the symbols have their usual meanings (Slichter, 1978), the solutions for the energies being:

$$E_m = -\gamma_n \hbar H_0 m + \frac{e^2qQ}{4} \cdot \frac{3\cos^2\theta - 1}{2}(3m^2 - 2) \qquad (4)$$

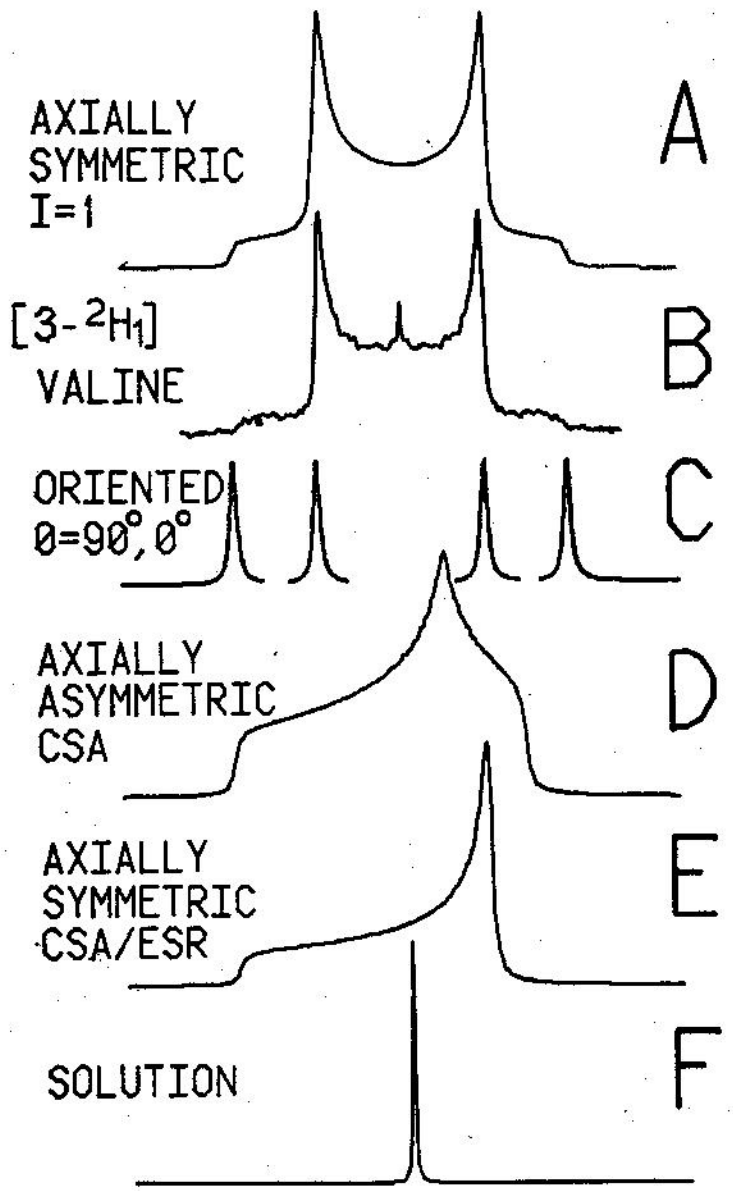

Fig. 1. *Theoretical and experimental lineshapes expected for ^{2}H-n.m.r., ^{13}C-n.m.r. and e.s.r. spectroscopy*

(A)Axially symmetric (I=1) lineshape (^{2}H-n.m.r.). (B) Experimental ^{2}H lineshape for [3-$^{2}H_1$] **valine** polycrystalline sample. (C) Oriented-sample ^{2}H-n.m.r. lineshape showing parallel and **perpendicular** edge absorptions. (D) Axially asymmetric chemical shift or e.s.r. lineshape. (E) **Axially** symmetric chemical shift or e.s.r. lineshape. (F) Solution n.m.r. lineshape.

The allowed transitions correspond to $+1 \leftrightarrow 0$ and $0 \leftrightarrow -1$ and give rise to a 'quadrupole splitting' of the absorption line, with separation between peak maxima of:

$$\Delta\nu = \frac{3}{2} \cdot \frac{e^2qQ}{h} \cdot \frac{3\cos^2\theta - 1}{2} \tag{5}$$

θ is the angle between the magnetic field H_0 and the principal axis of the electric field gradient tensor (frequently the C–D bond vector). All values of θ are possible for rigid polycrystalline solids and one therefore obtains a so-called 'powder pattern' (Fig. 1A) having a peak separation corresponding to $\theta = 90°$, for which $\Delta\nu = 3e^2qQ/4h$, and a shoulder separation corresponding to $\theta = 0°$, that is $\Delta\nu = 3e^2qQ/2h$. A typical experimental example, [3-^{2}H$_1$]valine, is shown in Fig. 1(B). A slightly modified version of eqn. (4) enables us to take into account motion of the group under consideration, such as a methyl group of valine spinning about its C_3 axis (see below). Eqn. (5) also indicates how we may determine the orientations of various groups in a protein crystal from ^{2}H n.m.r. spectra. For example, if a haem group labelled as ^{2}H at its α, β, γ and δ *meso*-positions were oriented in such a way in a crystal that the plane of the haem ring was at 90° to the external magnetic field H_0, then a 'sharp line' spectrum (Fig. 1C) having $\Delta\nu_Q$ approx. 138 kHz would be obtained, i.e., the splitting would correspond to three-quarters of the electric quadrupole coupling constant, which is approx. 184 kHz for aromatic systems (Barnes, 1974). Clearly then, it should therefore be possible to determine the orientation of a particular ^{2}H-labelled group in an ordered system from its quadrupole splitting ($\Delta\nu_Q$) and a knowledge of the breadth of the random powder pattern distribution. Similar information should also be extractable from ^{13}C n.m.r. chemical shift anisotropy powder patterns, which are shown schematically in Figs. 1(D) and 1(E). These lineshapes are also characteristics of axially asymmetric and axially symmetric electron spin resonance *g*-tensors, respectively.

Note that in solution, both the second rank tensor interactions described by $\mathcal{H}_Q$ and $\mathcal{H}_{CSA}$ are averaged to zero due to rapid particle tumbling, and conventional 'high-resolution' ^{2}H and ^{13}C spectra may be obtained (Oldfield *et al.*, 1975 *a*, *b*; Oldfield & Allerhand, 1975; Oldfield & Meadows, 1978; Oster *et al.*, 1975; Wooten & Cohen, 1979) as illustrated in Fig. 1(F).

Magnetic Ordering

Since we cannot easily grow sufficiently large single crystals for n.m.r. spectroscopy, it is clearly necessary to prepare highly oriented or ordered arrays of small crystals. Here, there are at least three possible approaches to obtaining such oriented samples: (i) magnetic ordering, (ii) electric ordering and (iii) mechanical ordering.

For a molecule or particle having a magnetic susceptibility χ, the magnetic energy in a field of intensity H is:

$$E = -\tfrac{1}{2} H \cdot \chi \cdot H \tag{8}$$

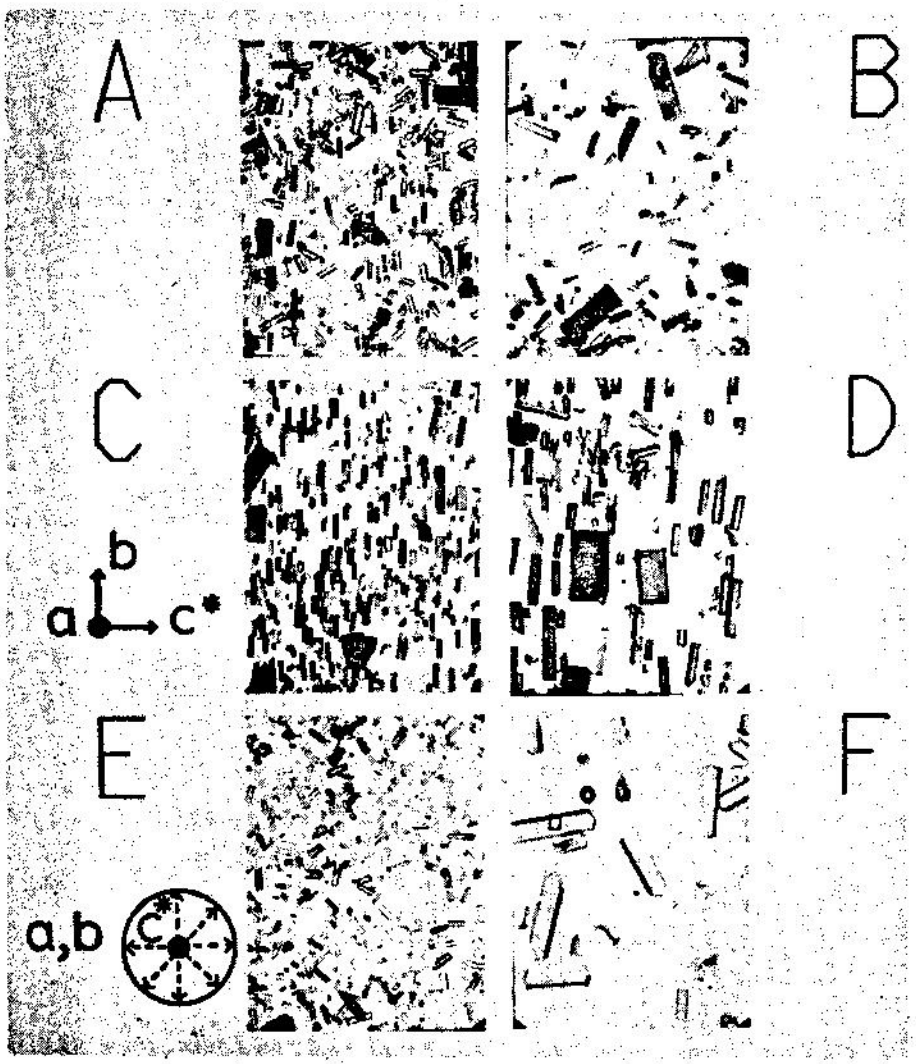

Fig. 2. *Photomicrographs of sperm whale (Physeter catodon) myoglobin microcrystals suspended in approx. 90%-satd. $(NH_4)_2SO_4$*

(A) Random microcrystals in the absence of a magnetic field, ×100 on a 5 inch × 4 inch Polaroid negative; (B) random microcrystals, ×200; (C) ordered microcrystals, ×100; (D) as (C) but ×200; (E) ordered protein microcrystals, ×100. The axis of ordering is perpendicular to the plane of the page and is approximately along the crystallographic c^* axis. (F) High power (×400) view of (E).

while for a similar particle having a dipole moment μ in an electric field of intensity F the energy is:

$$E = -\mu \cdot F \tag{9}$$

'Back of the envelope' calculations with typical protein dipole moments (Schlecht, 1969) of say 400 D, and magnetic susceptibilities (χ) corresponding

to e.s.r. g-values of, say, $g_{max.}$ approx. 3, $g_{min.}$ approx. 1, led us to believe that for even the smallest paramagnetic protein microcrystals (approx. 10^{-3} cm dimensions), it should be possible to make both the electric and magnetic interaction energies considerably in excess of the thermal energy kT (per particle). Unfortunately, however, the situation is not that simple, since occupation of upper Kramer's levels is expected in the case of many paramagnetic proteins of interest, and electric ordering experiments are technically difficult, even in the absence of the internal field problem (O'Konski *et al.*, 1959). Nevertheless, as we show below, paramagnetic protein microcrystals may be readily aligned by externally applied magnetic fields.

We show in Fig. 2 (Rothgeb & Oldfield, 1981) photomicrographs of a randomly oriented array of microcrystals of metaquomyoglobin (from sperm whale), crystallized from 3.2 M-$(NH_4)_2SO_4$, which have then been suspended in a dense (approx. 90%-satd.) $(NH_4)_2SO_4$ solution. Fig. 2(A) shows a wide-field view (× 100 on a 5 inch × 4 inch Polaroid negative) and Fig. 2(B) is from the same sample but at higher magnification (× 200) and includes several larger crystals (approx. 0.3 mm length). Careful inspection of Figs. 2(A) and 2(B) reveals two apparent crystal types: those with square ends and those with pointed ends. When the sample of Fig. 2 is placed for a few minutes in a d.c. magnetic field (H_0) of about 0.3 T strength, the protein microcrystals become highly ordered, aligning with their long axis perpendicular to the field direction, Figs. 2(C) and 2(D). Note that now all crystals appear to have square ends. Clearly then, the paramagnetic protein microcrystals are being aligned by the field, and must thus have their maximum (crystal) susceptibility along H_0 which, as shown in Figs. 2(C) and 2(D), corresponds to the crystallographic c^* axis along H_0. When viewed along the a-axis the crystal appears rectangular Figs. 2(C) and 2(D), but in a random powder distribution both views along c^* (pointed ends, Figs. 2A and 2B), a and b (square or rectangular, Figs. 2A and 2B) will be seen.

When we orient a sample suspended in a vertical microscope cavity-slide in a horizontal d.c. magnetic field of approx. 0.3 T, then remove it and view it in the normal horizontal fashion, the result is a view 'along' the field direction (Figs. 2E and 2F). Note that all crystals now appear 'capped' (in Fig. 2F) whereas all ends appear square in Fig. 1(D), the sample being disordered along c^*.

We show in Fig. 3 the effects of magnetic ordering on the ^2H n.m.r. spectra of sperm whale (*Physeter catodon*) myoglobin which has been specifically enriched as C^2H_3 at the *S*-methyl groups of Met-55 and Met-131 (Oldfield & Rothgeb, 1980; Rothgeb & Oldfield, 1981). In Fig. 3(A) we show the effect of magnetic ordering on the spectrum of metaquomyoglobin. The left-hand spectrum is broad and arises from a solid crystal powder, and it has a linewidth ($\Delta\nu_Q$) of about 31 kHz. At low temperatures, spectra having $\Delta\nu_Q$ of about 38 kHz are obtained. This splitting arises due to the averaging of the rigid-lattice quadrupole coupling constant (approx. 127 kHz; Barnes, 1974) by about a factor of three due to the approximately tetrahedral nature of the S^δ–C^ε–H^ε bond. The further reduction from 38 to 31 kHz at higher temperature (Fig. 3A) implies further motion of the methionine side chain, which may be quantitated (Rothgeb & Oldfield, 1981). Note that the spectrum in Fig. 3(A) also contains

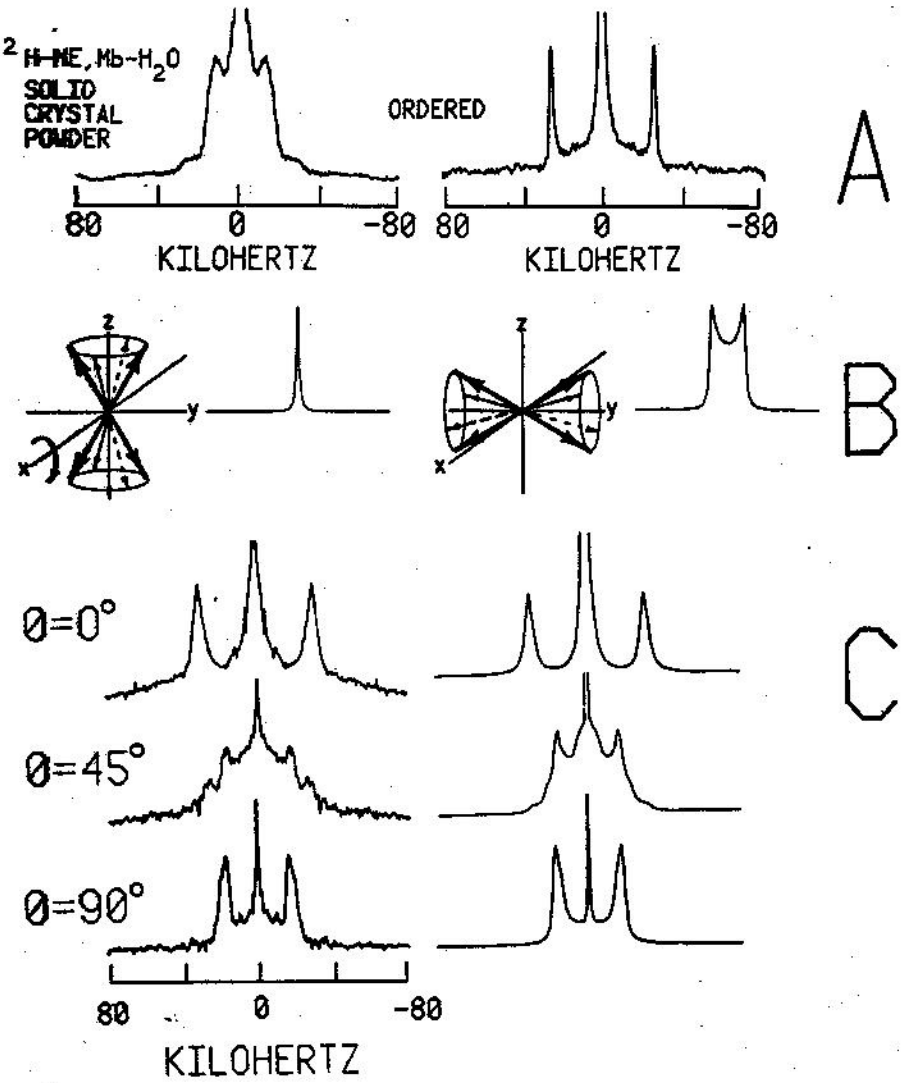

Fig. 3. *Experimental and computer-simulated ^{2}H-n.m.r. spectra of ^{2}H-labelled protein crystals*

(A) ^{2}H quadrupole-echo Fourier transform n.m.r. spectra at 55.3 MHz and 20 ± 2°C of [*methyl*-^{2}H]methionine-labelled sperm whale myoglobin as a solid hydrated crystal powder and a magnetically ordered sample, together with their spectral simulations. Solid crystal powder (left) hydrated with approx. 90%-satd. $(NH_4)_2SO_4$ (176685 scans, 65 ms recycle time, $\tau_1 = \tau_2 = 65$ μs, 7 μs 90° pulse widths, 167 kHz spectral width, 4K real data points, linebroadening 400 Hz). Magnetically ordered spectrum (right) after suspension in approx. 90%-satd. $(NH_4)_2SO_4$ (245839 scans, 65 ms recycle time, $\tau_1 = \tau_2 = 61$ μs, 7 μs 90° pulse widths, 167 kHz spectra width, 4K real data points, linebroadening 400 Hz). **(B)** Vector diagram and computer-simulated results showing the effects of sample rotation on ^{2}H-n.m.r. spectral appearance for an initial 'magic-angle' distribution of electric field gradient tensor principal components aligned along the field direction H_0. **(C)** Frozen-sample ^{2}H-n.m.r. rotation patterns of [*methyl*-^{2}H]methionine-labelled ferrimyoglobin from sperm whale, together with their computer simulations. Data acquisition conditions were typically: recycle time 65 ms, $\tau_1 = \tau_2 = 65$ μs, 7 μs 90° pulse widths, 167 kHz spectral width, 4K real data points, 400 Hz linebroadening due to exponential multiplication. The number of scans varied betwen 82615 and 262000. The spectral simulations assumed $\theta_1 = 17.5°$ and $\theta_2 = 54.6°$ and a linewidth of 2.8 kHz. The rotation angles are accurate to ± 3°.

a narrow central component; this arises from natural abundance HO^2H in the solvent.

When the solid crystal powder is resuspended in saturated $(NH_4)_2SO_4$ solution such that the crystals are floating in a medium of the same density, then the microcrystalline particles align as shown in Fig. 2, and the sharp 'ordered' spectrum seen in Fig. 3(A) is obtained. The 'ordered' spectrum of Fig. 3(A) has a $\Delta\nu_Q$ of 53.6 kHz, which is much greater than the approx. 40 kHz expected for only methyl-group rotation. The sharp spectrum clearly arises because of magnetic ordering, a 'pseudo single crystal' spectrum being obtained. From the magnitude of the quadrupole splitting in the magnetically ordered sample, it follows that the angle between the S^δ–C^ε bond vector and the axis of ordering (crystallographic c^*-axis) is 17.5 ± 2°. Additional unpublished experiments confirm the presence of a second peak in the centre of the spectrum arising from the second methionine group. It has a zero quadrupole splitting since it is oriented at the 'magic-angle' (54.7°) with respect to the axis of ordering. As noted below, these orientations are in excellent agreement with those calculated from the high resolution X-ray crystallographic structure (Takano, 1977). We also show later that addition of cyanide to these samples causes rotation of the crystals in the magnetic field, generating a new type of n.m.r. spectrum in which both methionine resonances may be resolved.

We show in Fig. 3(B) the effect expected theoretically of rotating a magnetically ordered sample after the sample has been frozen. The left-hand drawing in Fig. 3(B) shows the orientation of the C^δ–S^ε vectors in a magnetically ordered sample, which give rise to a simple sharp line spectrum due to 'magic-angle' orientation of the C–S vectors. When this sample is frozen and rotated about an axis orthogonal to that of ordering, a new n.m.r. spectrum is obtained, as shown in the right-hand drawing, Fig. 3(B). Computer lineshape simulation of this tilted conical distribution function leads to the broad lineshape containing a well resolved quadrupole splitting, (Fig. 3B). Such tilted lineshapes may, of course, be computed for any arbitrary initial vector orientations.

We have therefore frozen and carried out sample rotation experiments in our specifically deuterated myoglobin samples. We show in Fig. 3(C), on the left, spectra of ordered metaquomyoglobin (labelled as C^2H_3 at Met-55 and Met-131) for 0°, 45° and 90° rotations of the sample about an axis orthogonal to that of ordering. On the right-hand side of Fig. 3(C) we show theoretical computer-lineshape simulations, calculated assuming about 18° and 'magic-angle' (54.7°) orientations of the methionine S^δ–C^ε vectors. There is clearly good agreement between the experimental and theoretical simulations, supporting the assignment of one residue to the outer sharp splitting in Fig. 3(A), together with the presence of a sharp central 'magic-angle' component (Fig. 3A). A compilation of the experimental quadrupole splittings, and of the experimental and theoretical angles between the S^δ–C^ε vectors and the axis of ordering, is given in Table 1 (Rothgeb & Oldfield, 1981).

Table 1. *Derivation of structural information from quadrupole splitting data and assignment of resonances via spin-label titration and from crystallographic co-ordinates*

Data were obtained from the spectra in Fig. 3. Spectra were recorded and samples ordered at 8.5 T. The crystallographic co-ordinates were for sperm whale (*Physeter catodon*) metaquomyoglobin (Takano, 1977). The metaquomyoglobin was in the form of magnetically ordered microcrystals of approx. 0.1 mm dimensions (see Fig. 2) suspended in approx. 90%-satd. $(NH_4)_2SO_4$ at pH 6.4. The error in the quadrupole splitting is ± 500 Hz. The experimental angle is the angle between the principal axis of the electric field gradient tensor (assumed to be colinear with the S^{δ}–C^{α} bond vector) and the field direction, H_0. The error varies from ± 1° to ± 2° and is largest for angles most removed from the magic angle (54.7°). A quadrupole coupling of 31 kHz was used in the calculations.

	Quadrupole splitting ($\Delta\nu_Q$, kHz)	Experimental angle (θ,°)	Theoretical angle (θ,°)
Metaquomyoglobin	$53._6$*	$17._5$*	$16._6$†
	$0._0$‡	$54._7$‡	$53._4$§

* Assigned to Met-55 on the basis of spin-label titration experiments (Rothgeb & Oldfield, 1980; Jones *et al.*, 1976) and calculations from the crystal structure (Takano, 1977).
† Met-55 (Takano, 1977). The angle is between the S^{δ}–C^{α} bond vector and the crystallographic c^* axis.
‡ Assigned to Met-131. See * above.
§ Met-131. See † above.

Other Spectroscopic Techniques and Systems

The success of the magnetic ordering technique clearly should not be limited to observation of ^2H n.m.r. spectra of labelled high-spin ferric haem complexes. We have, therefore, investigated its application to ^{13}C n.m.r. and e.s.r., and have also investigated the ^2H n.m.r. of a variety of low-spin complexes. We show in Fig. 4 (A)the ^{13}C n.m.r. spectra of specifically ^{13}C enriched metaquomyoglobin (from sperm whale) in which we have this time incorporated ^{13}C labels at Met-55 and Met-131. The top spectrum in Fig. 4(A) shows the ^{13}C Fourier transform n.m.r. spectrum of magnetically ordered metaquomyoglobin. The two sharp features at about 10–15 p.p.m. from tetramethylsilane arise from the enriched [^{13}C]methionine methyl groups. In the absence of an intense proton decoupling field, or in the absence of the magnetic ordering effect, these resonances cannot be detected since they cover many hundreds of Hz. Both resonances are, however, well resolved in ordered systems under conditions of proton decoupling. The two sharp resonances may be even more clearly differentiated from the broad background of resonances in the 0–40 p.p.m. range by means of the convolution difference technique (Campbell *et al.*, 1973), as shown in the bottom spectrum of Fig. 4(A). Note that the chemical shift separation between the two resonances in the protein crystal is about 8.5 ± 1 p.p.m.; in solution these resonances have the same chemical shift (Jones *et al.*, 1975, 1976). The origin of the chemical shift difference lies at least in part in the different orientations of the groups in the protein crystal, which thereby places them in different parts of the ^{13}C chemical shift anisotropy powder pattern (Fig. 1E), but anisotropic hyperfine contributions may also contribute in the case of these relatively small effects.

Similar success is obtained when recording e.s.r. spectra of metaquomyoglobin at liquid-helium temperatures. We show in Fig. 4(B) a

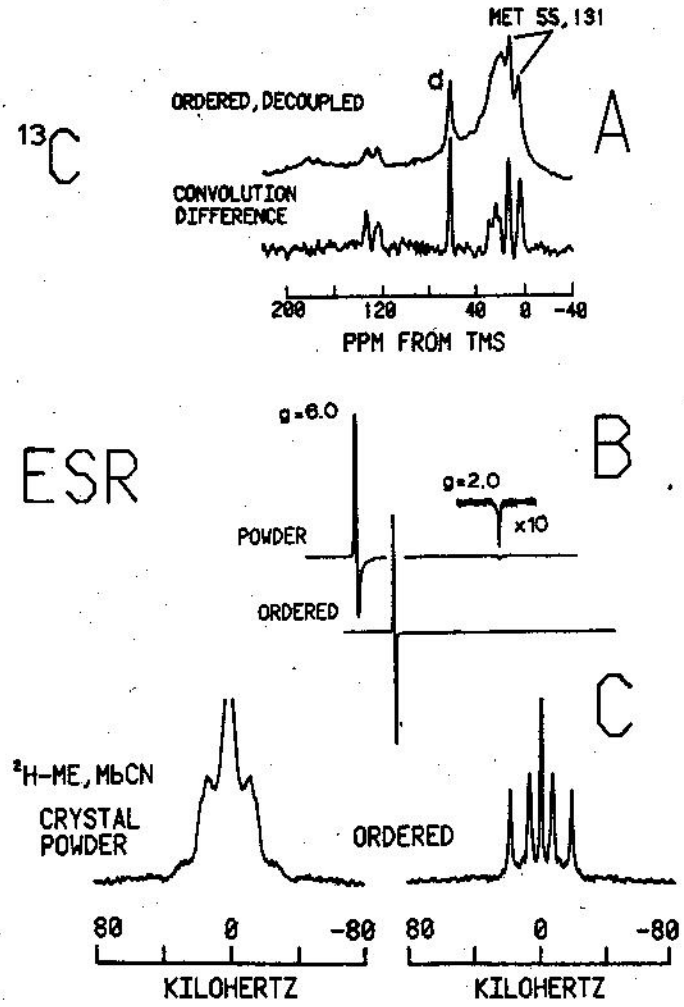

Fig. 4. *N.m.r. and e.s.r. spectra of sperm whale ferrimyoglobin*

(A) ^{13}C Fourier transform n.m.r. spectra (at 37.7 MHz) of [*methyl*-^{13}C] methionine-labelled sperm whale aquoferrimyoglobin microcrystals in a magnetically ordered sample, without and with application of the convolution-difference technique (Campbell *et al.*, 1973). (B) E.s.r. spectra obtained at 9.3 GHz of hydrated powder, and magnetically ordered sperm whale aquoferrimyoglobin microcrystals. (C) ^{2}H quadrupole echo Fourier transform n.m.r. spectra at 55.3 MHz and 22 ± 1°C of [*methyl*-^{2}H]methionine-labelled sperm whale cyanoferrimyoglobin. Left, solid powder sample hydrated with 90%-satd. $(NH_4)_2SO_4$, 233644 scans, 65 ms recycle time, $\tau_1 = \tau_2 = 65$ μs, 7 μs 90° pulse widths, 167 kHz spectral width, 4K real data points, linebroadening 400 Hz. Right, magnetically ordered cyanoferrimyoglobin suspended in approx. 90%-satd. $(NH_4)_2SO_4$, pH 6.4, 940703 scans, 61 ms recycle time, $\tau_1 = \tau_2 = 61$ μs, 9 μs 90° pulsewidths, 167 kHz spectral width, 4 K real data points, 400 Hz linebroadening.

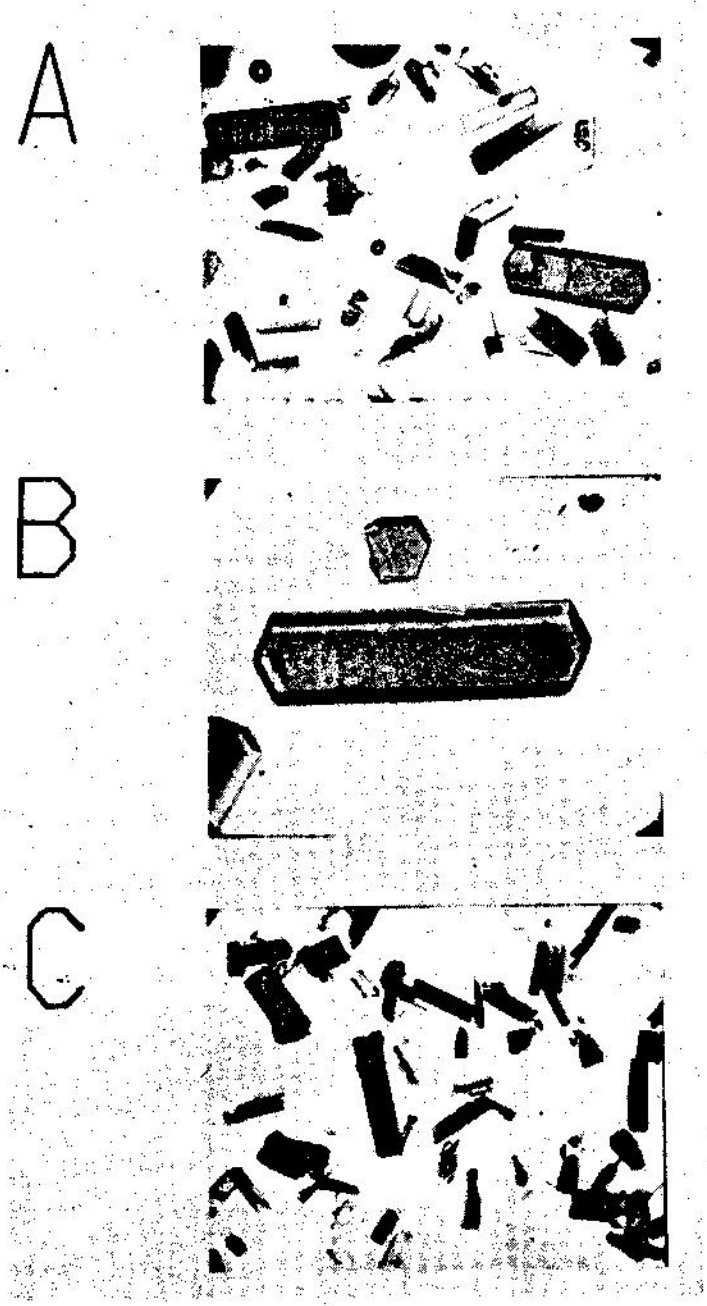

Fig. 5. *Photomicrographs of cyanoferrimyoglobin microcrystals suspended in approx. 90% satd. $(NH_4)_2SO_4$ at 24 ± 1°C*

(A) Random microcrystalline dispersion. ×100 on a 5 inch × 4 inch Polaroid negative. (B) Magnetically ordered microcrystals of cyanoferrimyoglobin, ×400. (C) 'Sideways ordered' view of magnetically ordered cyanoferrimyoglobin microcrystalline array.

powder-distribution e.s.r. spectrum of metaquomyoglobin and an e.s.r. spectrum of a magnetically ordered sample. The protein microcrystals were suspended in about 90% satd. $(NH_4)_2SO_4$, and were then ordered at about 0.9T, followed by rapid freezing, and then cooling to approx. 4K for e.s.r. spectroscopy. The sharp resonance occurs at a g-value of 6.0 (Fig. 4B, bottom) indicating that the crystals at high temperature must have been aligned along what is at low temperature the maximum g-value. This result indicates that even though upper Kramer's levels may be occupied at room temperature, contributing to the overall susceptibility of the protein, this effect does not defeat the magnetic ordering experiment.

In addition to this important observation, we note that such experiments are not limited solely to observations on high-spin ferric proteins. We present in Fig. 4(C) ^{2}H-n.m.r. spectra of the low-spin ferric haemoprotein cyanometmyoglobin, MbFe(III)(CN), labelled as C^2H_3 at Met-55 and Met-131. The samples in Fig. 4(C) were prepared by adding approx. 20 mg of KCN in saturated $(NH_4)_2SO_4$ to a sample of Type A($P2_1$) metaquomyoglobin crystals, followed by pH adjustment and a period of equilibration. The left-hand spectrum was obtained on a solid mass of crystals, obtained by removal of the mother liquor by filtration, although the crystals were still 'wet', and the spectrum obtained is not that characteristic of a dry powder. It may be simulated by using a quadrupole splitting ($\Delta\nu_Q$) of 33 kHz and a linewidth of 2.8 kHz. These simulation parameters are, as expected, very similar to those of the metaquomyoglobin sample. The sample of Fig. 4(C), when suspended in about 90%-satd. $(NH_4)_2SO_4$ solution, and immersed in a magnetic field of 8.5T, again orders very rapidly and the right-hand ^{2}H n.m.r. spectrum of Fig. 4(C) may be obtained. Note that this spectrum is completely different to that obtained for the high-spin metaquo complex (Fig. 3A). This result is to be expected since the low-spin electron g-tensor (Hori, 1971), and thus the magnetic susceptibility, are expected to be completely different both in magnitude and orientation to that of the high-spin species (Hori, 1971).

Photomicrographs of cyanoferrimyoglobin (MbCN) microcrystals [suspended in approx. 90% satd. $(NH_4)_2SO_4$, pH approx. 6.4] are presented in Fig. 5 and these show that cyanometmyoglobin crystals do indeed orient quite differently to those of metaquomyoglobin. We show in Fig. 5(A) a random distribution of MbCN crystals (× 200 on a 5 inch × 4 inch Polaroid negative) which is essentially identical to that obtained from a random distribution of metaquomyoglobin (MbH_2O), Figs. 2(A) and 2(B). Note in particular the dark crystal (viewed down a) and the large capped crystal (viewed down c^*). Upon magnetic ordering all crystals appear capped, and one large well-formed crystal and a crystal fragment are shown under high-magnification (× 400) in Fig. 5(B). On viewing down b, using the technique of sideways-ordering followed by a 90° sample rotation for photomicrography, the random distribution of square-ended crystals, Fig. 5(C), is produced. These results show conclusively that MbCN crystals orient approximately along a rather than c^*, although it does appear that the crystals may have a slight 'tilt'. It is worth mentioning at this point that diamagnetic (MbCO) crystals do not orient, as evidenced by ^{2}H n.m.r. at 8.5T, even at high fields. Calculations show, and experiments confirm, that once ordered these microcrystalline

arrays remained ordered for days, which leads to the possibility of preparing ordered systems at very high fields, and then carrying out numerous low- or zero-field (e.g., optical) experiments on these materials. If required, additional ordering may be achieved by the simple expedient of allowing the microcrystals to sediment out under the force of gravity. With metaquomyoglobin, for example, a two-dimensional array of crystals may be formed (our unpublished results).

An additional check of the mechanism of the magnetic ordering experiment, in addition to running spectra of diamagetic forms, is to prepare a protein where the transition metal centre is not expected to have additional close-lying Kramer's levels. This is frequently the case for the low spin d^7 ion Co(II). We have therefore prepared the Co(II) myoglobin derivative 'coboglobin' (Chien & Dickinson, 1972). The crystals (Chien & Dickinson, 1972) appear isomorphous with those of the ferric haem when grown from 3.2 M-$(NH_4)_2SO_4$.

Ordering along c^* rather than b is predicted for both metaquomyoglobin and deoxycoboglobin from examination of the respective g tensors (Chien & Dickinson, 1972; Dickinson & Chien, 1971). The angles of z, where z is the minimum g-value and is along the haem normal, with respect to a, b and c^* are 23°, 70° and 79° for deoxycoboglobin (Chien & Dickinson, 1972) and 21°, 68° and 88° for metmyoglobin (Dickinson & Chien, 1971). The minimum energy configuration will clearly be one in which the minimum g-value is at 90° to H_0. For both MbH_2O and CoMb this corresponds to H_0 close to c^*. This is what is observed experimentally for deoxycoboglobin, as shown in Fig. 6 where we show a sample of magnetically ordered crystals oriented along c^*.

Assignments, Dynamics and More Statics

Use of n.m.r. spectroscopic relaxation parameters to investigate the dynamic structure of protein crystals will, of course, rely on the correct assignment of individual-atom resonances. We have carried out such assignments for the methionine methyl groups in high and low-spin myoglobins by recourse to the X-ray determined crystal structures, and by use of paramagnetic spin-label probes to broaden surface residues. It has been shown previously that Met-55 is considerably more exposed than Met-131 (Jones *et al.*, 1976). Consequently, addition of the spin-label free-radical Tempamine to microcrystals of MbCN or MbH_2O causes a broadening of the resonance of the more exposed residue, Met-55. Addition of Tempamine to MbCN at a variety of pH values broadens the inner resonance, whereas addition of Tempamine to the high-spin metaquo form, or to fluoroferrimyoglobin, causes broadening of the outer resonance. These considerations, together with the known orientations of the methionine groups from the X-ray crystal structure, lead to a reasonably unequivocal assignment of both resonances.

Although we shall not go into detail of the relaxation of these groups in myoglobin at this time, we note that it is indeed very straightforward to measure the spin–lattice and spin–spin relaxation times of ^2H-labelled resonances in protein crystals. The resonances of the ^2H-labelled methionine

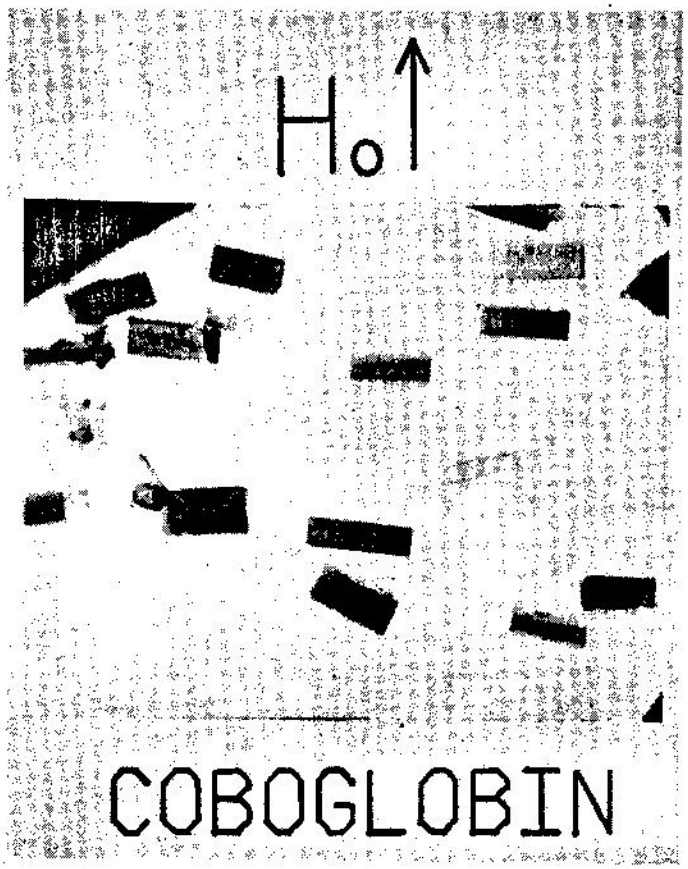

Fig. 6. *Photomicrograph of deoxycoboglobin microcrystals suspended in approx. 90%-satd. $(NH_4)_2SO_4$*

Sample was ordered for 1 h at 0.3 T. The axis of ordering is apparently very similar to that seen with metaquo (FeIII) myoglobin.

groups shown in Figs. 5, 3(A) and 4(C) have T_1 values of approx. 0.25 s (our unpublished results). It is now therefore a straightforward matter to determine the temperature dependence of these relaxation times in order to arrive at Arrhenius activation energies for the motional processes involved. These may then be compared with the values obtained for other residues, such as histidine, to determine in more detail the dynamics of amino acid side-chain motions in protein crystals using relatively direct methods. These parameters may also be used in comparisons with similar dynamic properties determined on proteins in membranes, and of proteins in solution.

We have recently used such ^2H n.m.r. relaxation measurements to investigate the dynamics of proteins dissolved in solution. We have been able to show that there is good agreement between the experimentally determined ^2H T_1 and T_2 values, and values calculated using electric quadrupole coupling constants determined from solid-state ^2H n.m.r. spectra and known rotational

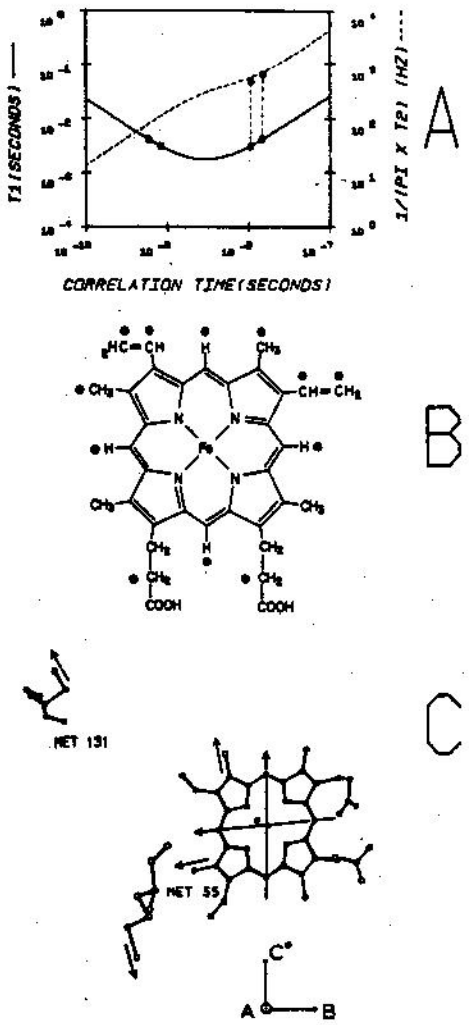

Fig. 7. *N.m.r. studies of lysozyme and metaquomyoglobin*

(A) Log–log plot of theoretical ^2H spin–spin (T_2) and spin–lattice (T_1) relaxation times as a function of rotational correlation time (τ_R) assuming an isotropic rotor model and an electric quadrupole coupling constant (e^2qQ/h) of 166 kHz. Experimental T_1 and T_2 values (●) for [^2H] histidine-labelled hen egg lysozome (EC 3.2.1.17) (6 mM in 200 mM-NaCl, pH 4.3 at 23°C and 62°C). (B) Structure of haem *b*, the prosthetic group of haemoglobin and myoglobin. The sites of ^2H label incorporation we have studied are indicated (●). (C) Partial static structure of metaquomyoglobin (Takano, 1977) showing the C–^2H vector orientations determined by ^2H-n.m.r. spectroscopy. There is a 90° uncertainty in the haem orientation, which may be resolved by means of one selective labelling experiment.

correlation times, both within and outside of the 'extreme narrowing limit' (our unpublished results). We show in Fig. 7(A) typical theoretical results for T_1 and linewidth calculated using standard relaxation theory (Abragam, 1961), for the case of a [^2H]histidine-labelled lysozyme, which has an amino acid e^2qQ/h approx. 166 kHz (our unpublished results) and a correlation time τ_R

approx. 12 ns (Oldfield *et al.*, 1975*a*). The experimental points (●) for T_1 (4.3, 3.2 ms) and linewidth (660, 440 Hz) are in good agreement with those predicted theoretically.

Such ^{2}H-labelled species are useful for determining other residue orientations in protein crystals, as shown in Figs. 7(B) and 7(C). We have therefore synthesized a wide variety of ^{2}H-labelled haems (Fig. 7B) and incorporated them into MbH_2O crystals for magnetic ordering experiments. We show in Fig. 7(C) the results of such experiments, where we have determined the C–^{2}H vector orientations, superimposed for clarity on the relevant part of the crystal structure (Takano, 1977). At present there is a 'phase' uncertainty about the haem orientation if only n.m.r. data is used, but this will be partially removed when a selectively ^{2}H-labelled haem is obtained. Both solution and solid ^{2}H-n.m.r. results (our unpublished results) indicate that there is essentially no motion of the haem in myoglobin.

It is perhaps worth emphasizing at this point that only the smallest crystals are required for these types of experiment, so that systems which have not yet been fully investigated by high resolution X-ray diffraction, due to the difficulty of forming adequate crystals, may be examined. For example catalase, peroxidase, chloroperoxidase and cytochrome *P*-450, may be well worth investigating with this technique. In addition, of course, the orientation of substrates, such as camphor binding to cytochrome *P*-450, may be determined in a very direct fashion with our techniques, and studies with additional systems are under way.

N.m.r. of Membrane Proteins

A major additional thrust of our research group at present involves the determination of the static orientation of amino acids in membrane proteins, together with a very detailed study of their molecular dynamics. We are investigating principally two cell membrane systems, that of *Acholeplasma laidlawii B* (PG9), and the purple membrane systems of the extreme halophile *Halobacterium halobium*. The first system has been chosen because of the ease of preparing relatively pure cell membranes, and the ease with which fatty acid, carotenoid and sterol content may be varied. Our goal here is to study protein–lipid interaction from the point of view of the most important membrane components, the membrane proteins. A second goal of our research in this area is to study the proton pumping system, bacteriorhodopsin, in the *Halobacterium* purple membrane. This system has been chosen because of the occurrence of only a single membrane protein in the purple membrane. Exceptionally encouraging n.m.r. results have been obtained with both systems, and we are currently investigating phenylalanine, tyrosine, tryptophan, glycine, alanine, valine, leucine and methionine amino acid dynamics. Our results (at 55.3 MHz) indicate the extreme rigidity, on a microsecond timescale, of many amino acid side chains in membrane proteins.

We show in Figs. 8(A) and 8(B) the ^{2}H n.m.r. spectra of [3-$^2H_1$]valine and [4-$^2H_6$]valine, in the solid state at room temperature. The spectrum of [$^2H_1$]-valine is characteristic of a system totally immobile on the timescale of the reciprocal of the anisotropy of the quadrupole coupling constant, that is to say

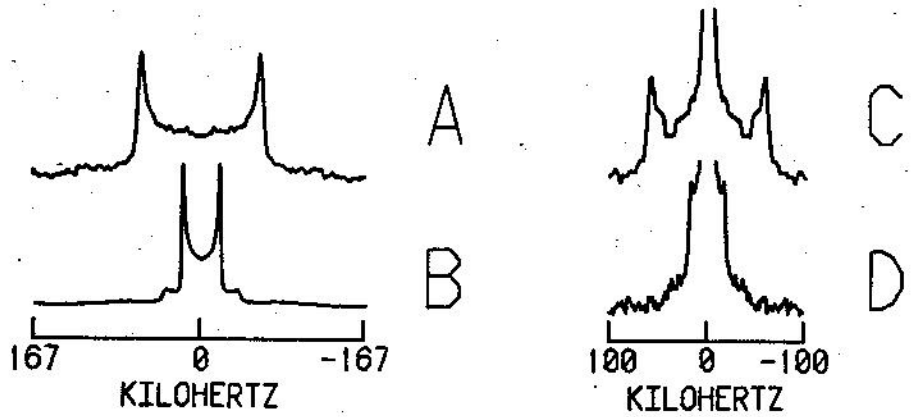

Fig. 8. *^2H Fourier transform n.m.r. spectra of specifically ^2H-labelled amino-acids, and specifically labelled biological membranes*

(A) [3-$^2H_1$]valine, 23°C; (B) [4-$^2H_6$]valine, 23°C; (C) [3-$^2H_1$]valine-enriched *Halobacterium halobium* purple membranes in water at 37°C. (D) [4-$^2H_6$]valine-enriched *Acholeplasma laidlawii* B (PG9) cell membranes in water at 25°C.

on an approximately 1 μs timescale. The full rigid lattice width of approx. 127.5 kHz, corresponding to a static quadrupole coupling constant e^2qQ/h of approx. 167 kHz, is manifest. In Fig. 8(B), however, we see the spectrum of the amino acid [4-$^2H_6$] valine, in which case fast methyl-group rotation has averaged the static quadrupole coupling constant by a value of $\frac{1}{2}(3\cos^2 109.5° - 1)$, i.e., by a factor of about 3, and a motionally averaged spectrum having a breadth of approx. 40 kHz is obtained. When we observe the ^2H Fourier transform n.m.r. spectra of membrane proteins, perhaps somewhat surprisingly, very similar spectra are obtained. In Fig. 8(C) we see the ^2H n.m.r. spectrum of *H. halobium* purple membranes enriched with [3-$^2H_1$]-valine. The results are very similar to those of Fig. 8(A) and indicate that there is little fast motion about the C^α– C^β bond of the protein's valine side-chains. This result is confirmed by spectra of [4-$^2H_6$]valine-labelled purple membranes (our unpublished results) and very similar results are obtained in the case of the *Acholeplasma* cell membrane (Fig. 8D). Observation of a motionally averaged quadrupole splitting of about 40 kHz (Fig. 8D) indicates unequivocally that there is only very fast motion about the C^β–C^γ bond in valine, and that motion about the C^α–C^β bond is slow on the n.m.r. timescale. If motion about C^α–C^β were fast, then a methyl group splitting of about 12 kHz would be obtained, i.e. the quadrupole splitting would have to be reduced by another factor of approx. 3. Observation of the 40 kHz methyl splittings, in fact, necessitates a splitting of about 125 kHz for the [3-$^2H_1$]valine, as is observed.

The picture of valine amino acid side-chain dynamics that arises from these experiments is therefore one in which the backbone of the protein is completely immobile on the microsecond timescale; motion about the C^α–C^β bond is probably slow, but motion about the C^β–C^γ bond is very fast. Given the extreme sensitivity of n.m.r. spectroscopy in determination of dynamics on a

wide variety of timescales, covering the picosecond to hundreds-of-seconds timescale range by use of appropriate relaxation techniques, these results strongly suggest that it will soon be possible to have a rather detailed picture of side chain and backbone dynamics of membrane proteins. Since many membranes may be ordered in strong magnetic fields (Neugebauer *et al.*, 1977), or by drying down on glass or mica slides, the way is now open to the determination of the orientation of many membrane protein amino acid side-chains, together with investigation of their dynamic properties.

Protein–Lipid Interaction

The idea that membrane proteins are solvated by a layer of immobilized boundary lipid was first put forward by Jost and coworkers (Jost *et al.*, 1973 *a,b,c,* 1977), originally for the cytochrome oxidase system, and subsequently for cytochrome b_5 (Dehlinger *et al.*, 1974) and sarcoplasmic reticulum ATPase (Jost & Griffith, 1978), and similar concepts have been presented by many other workers – notably the 'annulus' of Metcalfe and coworkers (Warren *et al.*, 1974 *a,b,* 1975; Hesketh *et al.*, 1976), the 'halo' of Stier & Sackmann (1973), together with several additional examples from other groups (Caron *et al.*, 1974; Grant & McConnell, 1974; Cornell *et al.*, 1978; Marsh *et al.*, 1978). In almost all instances, the overwhelming evidence for rigid or immobilized 'boundary lipid' comes from the 'rigid glass' (long correlation time) e.s.r. spectrum of a nitroxide free-radical introduced into the system. The general conclusion from many of these and other theoretical studies (Marčelja, 1976; Schröder, 1977; Scott & Cherng, 1978) is that proteins increase order greatly for the first layer of lipid adjacent to protein, and that significant perturbations exist for the second and perhaps the third layer of lipid.

There are, however, problems associated with the interpretation of the e.s.r. data in terms of specific molecular models. The first problem concerns the interpretation of the e.s.r. spectra themselves. The 'boundary lipid' spectra actually only demonstrate the fact that the spin-label is immobilized by the protein, that is to say the correlation time of the label increases. There is no information indicating that boundary lipids are ordered (as they are by for example cholesterol), and indeed the orientation experiments of Jost *et al.* (1973*b*) actually show a random distribution of boundary lipid spin labels on the protein surface. A second problem is that, if one is to have confidence in the e.s.r. results, then one must be sure that the spin-labelled lipid behaves in exactly the same way as a non-labelled lipid would in its interaction with protein. However, the e.s.r. spin-label studies by Jost and coworkers have indicated that the spin-label binding sites on the hydrophobic segment of cytochrome b_5 (Dehlinger *et al.*, 1974) and sarcoplasmic reticulum ATPase molecules (Jost & Griffith, 1978) are significantly more polar than the interior of a phospholipid bilayer, as judged by the values of the hyperfine coupling constant, which Jost and coworkers have suggested is due to hydrogen bonding between the polypeptide and the N–O moiety of the spin label (Dehlinger *et al.*, 1974). Since normal membrane lipids do not possess polar isoxazolidine or nitroxide groups, then the possibility exists that spin-labels may preferentially

bind to proteins in a bilayer, and may be selectively immobilized. We have therefore applied the non-perturbing technique of ^{2}H n.m.r. spectroscopy to a study of these problems in the hope of effecting some resolution of the problem.

Early studies demonstrated that addition of cholesterol to a ^{2}H-labelled DMPC bilayer at 1 : 1 molar ratio caused an increase of almost a factor of two in the order parameter of the lipid hydrocarbon chain, corresponding to an increase in ^{2}H quadrupole splitting from about 27 kHz to about 49 kHz (at 30°; Oldfield *et al.*, 1971). Below the phase transition temperature of the pure lipid, the hydrocarbon chains were prevented by cholesterol from crystallizing into the rigid α-crystalline gel state, and the observed quadrupole splitting remained at about 50 kHz even at 10°C, some 13°C below the gel-to-liquid-crystal phase transition temperature. These effects seen with ^{2}H n.m.r. were precisely those predicted on the basis of earlier calorimetric studies (Ladbrooke *et al.*, 1968) and ^{1}H n.m.r. of sonicated vesicles (Chapman & Penkett, 1966).

The effects of proteins on the ^{2}H n.m.r. spectra of hydrocarbon-chain-labelled phospholipids are predicted, by the use of the boundary lipid idea, to be an increase in ^{2}H n.m.r. quadrupole splittings (or order parameters) of lipid associated with protein (Hong & Hubbell, 1972; Marčelja, 1976; Jost & Griffith, 1978; Marsh *et al.*, 1978; Scott & Cherng, 1978). We show in Fig. 9(A) results obtained with cytochrome oxidase (EC 1.9.3.1) and sarcoplasmic reticulum ATPase (EC 3.6.1.3), the systems most frequently studied with physical techniques (Jost *et al.*, 1973 *a,b,c*, 1977; Longmuir *et al.*, 1977; Dahlquist *et al.*, 1977; Warren *et al.*, 1974 *a,b*, 1975; Hesketh *et al.*, 1976; Jost & Griffith, 1978; Marsh *et al.*, 1978; Moore *et al.*, 1978; Oldfield *et al.*, 1978*a*; Rice *et al.*, 1979*a*), together with the much smaller model system beef brain myelin proteolipid apoprotein (Papahadjopoulos *et al.*, 1975; Curatolo *et al.*, 1977; Rice *et al.*, 1979*b*). All systems were 'complexed' or 'reconstituted' with DMPC bilayers specifically deuterated at the terminal methyl position of the *sn*-2 chain, using standard techniques (Warren *et al.*, 1974*a,b*; Curatolo *et al.*, 1977; Oldfield *et al.*, 1978*a*), with particular emphasis being placed on total detergent or solvent removal (Oldfield *et al.*, 1978*a*; Rice *et al.*, 1979*a,b*). For comparison, also included is a ^{2}H-n.m.r. spectrum showing the effect of cholesterol, the sample again being made by standard techniques (Oldfield *et al.*, 1978*b*).

As may be seen from spectra in Fig. 9(A) the effect of incorporating protein into the lipid bilayer is to cause a decrease in order parameter (quadrupole splitting) of the ^{2}H-labelled methyl group, a disordering rather than an ordering effect. Similar effects are seen with a wide range of other proteins e.g. cytochrome b_5 (Oldfield *et al.*, 1978*a*) bacteriophage f1 coat protein (Oldfield *et al.*, 1978*a*) and mellitin (E. Oldfield & M. Meadows, unpublished results) with DMPC, as well as with other saturated and unsaturated phospholipids (Oldfield *et al.*, 1978*a*; Rice *et al.*, 1979*a,b*). The disordering effect is therefore not restricted to phosphatidylcholine molecules containing C_{14} saturated hydrocarbon chains although it is largest at the chain terminus (Rice *et al.*, 1979*b*; Kang *et al.*, 1979*a*; Kang *et al.*, 1981).

Cholesterol, on the other hand, causes a large increase in quadrupole

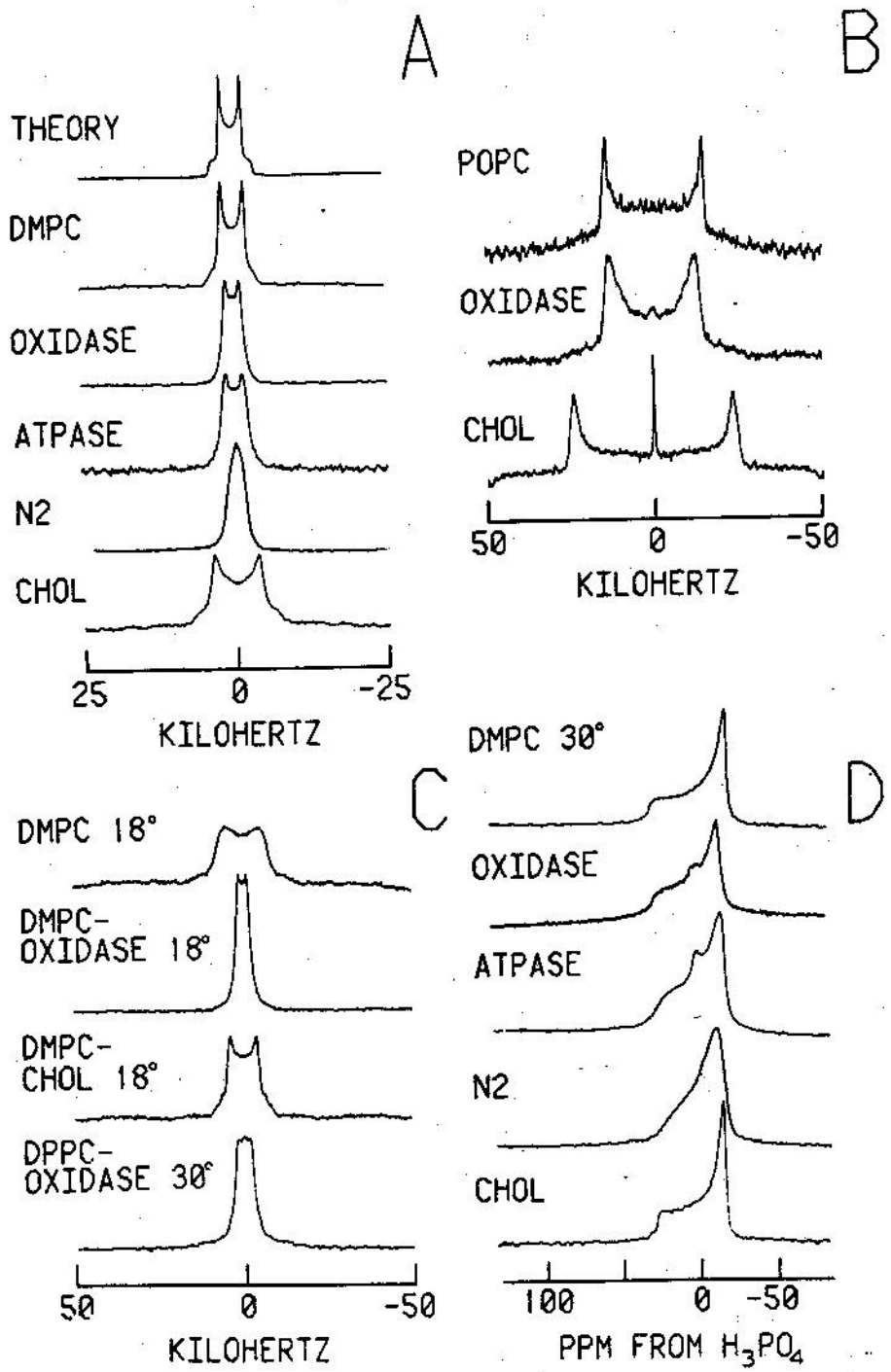

Fig. 9. *N.m.r. studies of phospholipids*

(A) Theoretical and experimental ^2H spectra of ^2H-labelled lipids showing the effects of proteins and cholesterol on hydrocarbon chain order. The top spectrum shows the theoretical lineshape. Below are shown spectra of DMPC and DMPC + approx. 65% (w/w) of the indicated protein (Oldfield *et al.*, 1978), and of approx. 33% (w/w) cholesterol. ^2H n.m.r. spectra were obtained

with the quadrupole-echo Fourier transform method at 5.2 T (corresponding to a ^2H resonance frequency of 34 MHz) on a homebuilt instrument. Sample size was typically 200 μl. (B) ^2H n.m.r. spectra of the unsaturated lipid, 1-[6-$^2H_2$]palmitoyl-2-oleoyl-*sn*-glycero-3-phosphocholine (POPC), showing the effects of protein and cholesterol on chain order near the polar interface. The top spectrum is of POPC in excess water at 30°C, the next spectrum is of a sample which contains 67% (w/w) cytochrome oxidase, and the final spectrum is of a sample which contains 33% (w/w) cholesterol. (C) ^2H n.m.r. spectra of phospholipids below their gel-to-liquid-crystal phase transition temperatures (T_c) showing the effects of protein and cholesterol on hydrocarbon chain organization. The protein containing sample consisted of approx. 65% (w/w) protein, the cholesterol containing sample contained about 33% (w/w) cholesterol. All samples were in excess ^2H-depleted water. (D) ^{31}P-n.m.r. spectra of DMPC in the presence of a variety of proteins, and of cholesterol. Sample conditions were as in (A). Spectra were recorded at 60.7 MHz using the Fourier transform method, and were fully proton-decoupled. N2 is the proteolipid apoprotein of myelin.

splitting or order parameter, consistent with its well known 'condensing' or ordering effect. Quantitatively, the order parameter of the DMPC 2-chain terminal methyl group decreases about 25% upon addition of approx. 70% by wt. of oxidase or ATPase ($\Delta\nu_Q$ decreases from 3.4 to approx. 2.6 kHz), but increases over 200% upon addition of 33% by wt. of cholesterol ($\Delta\nu_Q$ increases from 3.4 to 7.6 kHz; Oldfield *et al.*, 1978*b*; Jacobs & Oldfield, 1978) Above T_c the effects of each of the proteins we have investigated is to cause a decrease in $\Delta\nu_Q$, or even a collapse in quadrupole splitting as is seen with the proteolipid apoprotein (Fig. 9A) or in the case of gramicidin A' (Rice & Oldfield, 1979). Notably, e.s.r. studies of these samples in our laboratories have confirmed that highly immobilized nitroxide spin-label spectra are nevertheless obtained. These results may be rationalized either by invoking a specific nitroxide–protein interaction as suggested by Dehlinger *et al.* (1974) or by taking timescale differences between the ^2H-n.m.r. and e.s.r. into account.

In either case, however, one effect of protein (or polypeptide) on hydrocarbon chain methyl group order in phosphatidylcholine model systems must be to disorder (fluidize, mobilize) the chain terminus. Since no two-component spectra have been seen above the pure lipid phase transition temperature over a wide concentration range (our unpublished results) then exchange between 'bound' and 'free' lipid must be fast, in fact $\gtrsim 10^3$–10^4 s^{-1}.

Similar effects are seen when using more 'physiological' lipids such as the monounsaturated phosphatidylcholine, 1-[6-$^2H_2$]palmitoyl-2-oleoyl-*sn*-glycero-3-phosphatidylcholine ([6-$^2H_2$]POPC) in its liquid crystalline phase at 30°C. We show in Fig. 9(B) results that indicate that, as viewed from near the 'top' of this hydrocarbon chain, cytochrome oxidase has little effect on chain order, but cholesterol again causes a very large ordering (Rice *et al.*, 1979*a*). Essentially identical results are obtained when a C-6 labelled saturated phosphatidylcholine (DMPC) is used (Kang *et al.*, 1979*a*). There are therefore no gross differences between the interactions of liquid crystalline saturated and unsaturated phospholipids with the cytochrome oxidase molecule. Both lipids have their hydrocarbon chain order slightly decreased near the chain terminus owing to interaction with protein, whereas cholesterol causes a large increase in order at all chain positions.

At temperatures below that of the gel-to-liquid-crystal phase transition we find that both cholesterol and proteins prevent lipid hydrocarbon chains from crystallizing, as shown in Fig. 9(C). However, the cholesterol-containing

samples are far more ordered than those containing protein. At 30°C the lipid (a terminal methyl-labelled DMPC) is in the fluid liquid crystalline state and a well resolved quadrupole splitting ($\Delta\nu_Q$ 3.4 kHz) is observed. Cooling the pure lipid sample below the gel-to-liquid-crystal phase transition temperature (T_c) of about 23°C results in a large increase in quadrupole splitting at the phase transition temperature, the quadrupole splitting being approx. 15 kHz at 18°C (Fig. 9C). Incorporation either of protein (in this case cytochrome oxidase) or of cholesterol at high weight ratios into the lipid bilayer prevents crystallization of the lipid hydrocarbon chains into the rigid crystalline gel state, and the relatively narrow spectra of Figs. 9(A) and 9(C) are obtained. Note, however, that the cholesterol-containing sample has an order parameter at least twice that of the protein-containing samples. These results, together with those of Figs. 9(A) and 9(B), clearly lead to a model of protein–lipid interaction in which proteins may disorder the packing of lipid hydrocarbon chains, thereby decreasing the appropriate order parameter, at least near the terminal methyl end of the hydrocarbon chain. Cholesterol, on the other hand, orders the packing of lipid hydrocarbon chains above T_c at all positions, but, as with protein, disorders (relative to the gel state) below T_c by preventing hydrocarbon chain crystallization.

These effects must clearly be related to the structures of the perturbing molecules, the proteins and cholesterol. It seems to us to be most likely that the rough, irregular surfaces of proteins (with their 20 different amino-acid side-chains) cause lipid hydrocarbon chains to pack in a disordered way into 'vacancies' created by the side chains, and perhaps created in a time-dependent way by rotation and internal motions of the protein. Cholesterol, on the other hand, is a rigid tetracyclic structure, and inspection of molecular models reveals that it has rather planar sides, at least on the scale of a C–C bond length. Cholesterol acts as the rigid boundary of the theoretical protein–lipid interaction calculations (Kleemann & McConell, 1976; Marčelja, 1976; Schröder, 1977, Scott & Cherng, 1978; Owicki *et al.*, 1978), and prevents chain tilt, rotation and *gauche–trans* isomerization above T_c, and inhibits crystallization into the ordered gel phase below T_c. Below T_c in the presence of cholesterol, the lipid hydrocarbon chains are highly ordered (Oldfield *et al.*, 1971, 1978*b*; Gally *et al.*, 1976), the order parameter approaching $S=1.0$ at low temperatures (Gally *et al.*, 1976; Rice *et al.*, 1979*b*), although cholesterol still causes the bilayer to be disordered relative to the gel-state, since fast chain motion about the long axis is absent in the gel phase but is present in high-cholesterol-containing samples. In the presence of protein, the lipid hydrocarbon chains remain disordered due to the proximity of the rough or irregular protein surface, but at sufficiently low temperatures, the chains may begin to crystallize, presumably forming patches of protein-free lipid.

Although the order of the lipid hydrocarbon chains is in many cases clearly decreased by addition of protein, it is almost certain that the actual rates of motion of the lipid hydrocarbon chains become slower. In general, in n.m.r. spectroscopy, as the rate of motion of a group decreases then the width of the particular resonance line associated with the group increases, due to more effective relaxation. Although it is not yet a simple matter to calculate the ^{2}H-n.m.r. spectra of membranes, we have found in several instances that the ^{2}H-

n.m.r. linewidths of protein (or polypeptide) lipid complexes are larger than in the pure lipid bilayers, although the quadrupole splittings remain approximately the same. We have observed these effects with cytochrome oxidase, and with intact biological membranes using ^{2}H-n.m.r. (Kang *et al.*, 1979*b*) as well as with ^{31}P-n.m.r. in some systems (Rajan *et al.*, 1981). These results suggest that boundary lipid, as well as being somewhat disordered and mobile on the ^{2}H-n.m.r. timescale (2×10^{-5} s), nevertheless may in some cases undergo more effective relaxation in the presence of protein, due to increased correlation times.

^{31}P-N.m.r. of Protein–Lipid Interactions

^{31}P-n.m.r. of the gel and liquid crystalline states of a variety of phospholipids, together with the effects of cholesterol on headgroup molecular motion, have already been investigated by a number of investigators (Barker *et al.*, 1972; Yeagle *et al.*, 1975; Cullis & deKruyff, 1976; Kohler & Klein, 1976; Griffin, 1976; Brown & Seelig, 1978) so it is therefore of some interest to compare these results with our recent ^{31}P-n.m.r. studies of protein–lipid interactions.

We show in Fig. 9(D) selected results from a series of ^{31}P-n.m.r. experiments recently carried out in our laboratory which show that addition of protein (or polypeptide) to a phosphatidylcholine bilayer cause a decrease in $\Delta\sigma$ of the lipid phosphate group. For example, addition of sarcoplasmic reticulum ATPase or cytochrome oxidase to a DMPC bilayer reduces $\Delta\sigma$ from about 50 p.p.m. to about 45 p.p.m. (with 67% protein by wt.), whereas addition of high levels of proteolipid apoprotein cause even larger decreases. We also find that the spectral linewidths increase on addition of protein. These results suggest that in many cases lipid polar headgroups may interact directly with membrane proteins, and that as a result the headgroup phosphate motion may become slower and more isotropic. Spin-echo T_2 relaxation measurements of both pure lipid and protein–lipid complexes reveal rather anisotropic relaxation through the ^{31}P powder pattern, with proteins decreasing both T_1 and T_2 from their pure lipid values by a factor of 3 or 4, with 67% protein by wt. The headgroups therefore seem to be 'immobilized' by protein. Cholesterol also decreases $\Delta\sigma$ (Brown & Seelig, 1978) but in this case there are no large changes in T_1 or T_2 from the values found in pure lipid bilayers. This result indicates that cholesterol simply acts as an inert spacer molecule, there being no evidence for any sterol–lipid interaction.

The preceding results when taken together suggest to us that a major effect of proteins on hydrocarbon chain organization in both model and intact biological membranes is to cause a slight chain disordering. This effect is largest at the methyl end of the chain, is the opposite of that seen with the rigid cholesterol molecule, and is contrary to the idea of a rigid, ordered, boundary layer lipid surrounding membrane proteins. Boundary or annular lipids are probably rather disordered and fluid, these factors being important for enzyme activity.

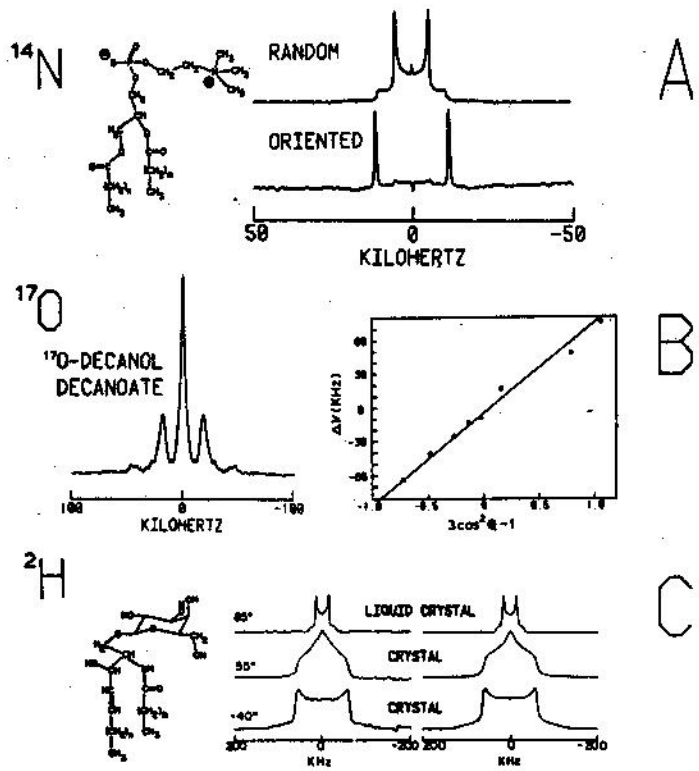

Fig. 10. *^{14}N, ^{17}O and ^{2}H n.m.r. spectra of some lipid bilayer systems*

(A) ^{14}N spectra of DMPC random dispersion in excess water at 30°C (top) together with oriented sample spectrum (of egg-lecithin, bottom) showing $\theta = 0°$ orientation. The quadrupole splitting observed is approx. 10 kHz (Siminovitch *et al.*, 1980). A typical phosphatidylcholine structure is shown. (B) ^{17}O n.m.r. spectrum, and rotation plot, for ^{17}O-enriched decanol in an oriented decanol/decanoate/water mesophase. By using oriented samples, it is possible to study systems whose quadrupole couplings are approx. 1 MHz. (C) ^{2}H Fourier transform n.m.r. spectra of ^{2}H-chain-labelled cerebroside, a galactosphingolipid (structure shown) in the liquid crystal phase in excess water (85°C, top spectrum, $\eta = 0$) and in the crystalline or gel phase (55°C, −40°C, bottom two spectra). A non-zero asymmetry parameter is obtained at 55°C due to fast rotational transitions in the hydrocarbon chain.

'New' Nuclei and 'New' Motions

In this part of our paper we would like to present some n.m.r. results with 'new' nuclei, and also present spectra characteristic of some new types of motions in lipid hydrocarbon chains. We show first in Fig. 10(A) results of ^{14}N-n.m.r. experiments carried out at natural abundance and 8.5 T, on a random powder of liquid crystalline phospholipid (top) and on a mechanically ordered (on glass slides) sample (bottom). The top spectrum shows a characteristic (spin $I = 1$ and asymmetry parameter $\eta = 0$) powder pattern for the ^{14}N nucleus in the phospholipid DMPC, and in the lower spectrum we show a sample of egg lecithin oriented on glass slides. The spectra may be fully understood by reference to Fig. 1, which illustrates the formation of the narrow line doublet spectrum for a single ($\theta = 0°$) orientation. This result

demonstrates unequivocally that the axis of motional averaging of the ^{14}N quadrupole interaction is the bilayer normal, as has been demonstrated previously for ^{31}P- and ^{2}H-n.m.r. studies of phospholipid headgroups. Observation of ^{14}N n.m.r. spectra opens the way to further clarification of the details of phospholipid headgroup motion in model and biological membrane systems. In Fig. 10(B) we present the first ^{17}O-n.m.r. spectra of lipid bilayer systems. Observation of ^{17}O in natural abundance in lipid bilayers is perhaps not feasible at the present time, so we have therefore synthesized a variety of ^{17}O-enriched species. Detection of ^{17}O resonances are, of course, particularly difficult because the quadrupole coupling constants are expected to be several MHz, resulting in spectral widths of perhaps 0.5 MHz. We have therefore produced samples oriented on glass slides, and carried out rotation plots near the 'magic-angle'. The plots of quadrupole coupling versus $(3\cos^2\theta-1)$ permits a determination of the effective quadrupole coupling constant in the system under investigation, and this type of experiment when extended to the ^{17}O nucleus in the phospholipid phosphate backbone is certain to yield valuable new information on phopholipid headgroup conformation. We have pointed out previously that complete knowledge of ^{2}H-, ^{13}C-, ^{14}N-, ^{17}O- and ^{31}P-n.m.r. spectra is required for an adequate analysis of phospholipid conformations in biological membranes (Skarjune & Oldfield, 1979).

Finally, we would like to show in addition to some 'new nuclei', some 'new' lineshapes, recently observed in glycolipid bilayer systems, which illustrate that 'specialized' motions may be readily detected by n.m.r. spectroscopy. The results of Fig. 10(C) show that asymmetry parameter $\eta = 1$ lineshapes may in some circumstances be obtained from lipid bilayer systems. In this instance, it appears that a two-site jump over a tetrahedral bond angle, due probably to some type of *gauche–trans* isomerization, is responsible for the observed lineshapes. Similar unusual non-zero asymmetry-parameter lineshapes are in general always to be expected for any such specialized two-fold motions. *Gauche–trans* isomerization is one example of such a specialized motion, and a second type of motion we have obtained evidence for involves the two-fold flipping of aromatic rings, in which case lineshapes of asymmetry parameter η approx. 0.6 are obtained (our unpublished results).

This work was supported by the U.S. National Institute of Health (grants CA-00595, HL-19481), by the U.S. National Science Foundation (grants PCM 78-23021, PCM 79-23170) and the Alfred P. Sloan Foundation, by the Los Alamos Scientific Laboratory Stable Isotope Resource, which is jointly supported by the U.S. Department of Energy and the U.S. National Institutes of Health (grant RR-99962), and by the University of Illinois NSF Regional Instrumentation Facility (grant CHE 79-16100). E.O. is an Alfred P. Sloan Foundation Fellow and a U.S.P.H.S. Research Career Development Awardee. T.M.R. is a National Science Foundation Postdoctoral Fellow.

References

Abragam, A. (1961) *The Principles of Nuclear Magnetism*, Clarendon Press, Oxford
Artymiuk, P.J., Blake, C.C.F., Grace, D.E.P., Oatley, S.J., Phillips, D.C. & Sternberg, M.J.E. (1979) *Nature (London)* **280**, 563–568
Barker, R.W., Bell, J.D., Radda, G.K. & Richards, R.E. (1972) *Biochim. Biophys. Acta* **260**, 161–163
Barnes, R.G. (1974) *Adv. Nucl. Quadrupole Reson.* **1**, 335–355
Blundell, T.L. & Johnson, L.N. (1976) *Protein Crystallography*, Academic Press, New York
Brown, M.F. & Seelig, J. (1978) *Biochemistry* **17**, 381–384
Campbell, I.D., Dobson, C.M., Williams, R.J.P. & Xavier, A.V. (1973) *J. Magn. Reson.* **11**,172–181
Caron, F., Mateu, L., Rigny, P. & Azerad, R. (1974) *J. Mol. Biol.* **85**, 279–300
Chance, B. (1966) in *Hemes and Hemoproteins* (Chance, B., Estabrook, R.W. & Yonetani, T., eds.) pp. 213–220, Academic Press, New York
Chapman, D. & Penkett, S.A. (1966) *Nature (London)* **211**, 1304–1305
Chien, J.C.W. & Dickinson, L.C. (1972) *Proc. Natl. Acad. Sci. U.S.A.* **69**, 2783–2787
Cornell, B.A., Sacré, M.M., Peel, W.E. & Chapman, D. (1978) *FEBS Lett.* **90**, 29–35
Cullis, P.R. & deKruyff, B. (1976) *Biochim. Biophys. Acta* **436**, 523–540
Curatolo, W., Sakura, J.D., Small, D.M. & Shipley, G.G. (1977) *Biochemistry* **16**, 2313–2319
Dahlquist, F.W., Muchmore, D.C., Davis, J.H. & Bloom, M. (1977) *Proc. Natl. Acad. Sci. U.S.A.* **74**, 5435–5439
Dehlinger, P.J., Jost, P.C. & Griffith, O.H. (1974) *Proc. Natl. Acad. Sci. U.S.A.* **71**, 2280–2284
Dickinson, L.C. & Chien, J.C.W. (1971) *J. Am. Chem. Soc.* **93**, 5036–5040
Dwek, R.A. (1973) *Nuclear Magnetic Resonance in Biochemistry: Applications to Enzyme Systems*, Clarendon Press, Oxford
Frauenfelder, H., Petsko, G.A. & Tsernoglou, D. (1979) *Nature (London)* **280**, 558–563
Gally, H.U., Seelig, A. & Seelig, J. (1976) *Hoppe-Seyler's Z. Physiol. Chem.* **357**, 1447–1450
Grant, C.W.M. & McConnell, H.M. (1974) *Proc. Natl. Acad. Sci. U.S.A.* **71**, 4653–4657
Griffin, R.G. (1976) *J. Am. Chem. Soc.* **98**, 851–853
Gurd, F.R.N. & Rothgeb, T.M. (1979) *Adv. Protein Chem.* **33**, 73–165
Hesketh, T.R., Smith, G.A., Houslay, M.D., McGill, K.A., Birdsall, N.J.M., Metcalfe, J.C. & Warren, G.B. (1976) *Biochemistry* **15**, 4145–4151
Hong, K. & Hubbell, W.L. (1972) *Proc. Natl. Acad. Sci. U.S.A.* **69**, 2617–2621
Hori, H. (1971) *Biochim. Biophys. Acta* **251**, 227–325
Jacobs, R. & Oldfield, E. (1978) *Biochemistry* **18**, 3280–3285
Jones, W.C., Jr., Rothgeb, T.M. & Gurd, F.R.N. (1975) *J. Am. Chem. Soc.* **97**, 3875–3877
Jones, W.C. Jr., Rothgeb, T.M. & Gurd, F.R.N. (1976) *J. Biol. Chem.* **251**, 7452–7460
Jost, P.C. & Griffith, O.H. (1978) in *Cellular Function and Molecular Structure: A Symposium on Biophysical Approaches to Biological Problems* (Agris, P.F., Loeppky, R.N. & Sykes, B.D., eds.), pp. 25–54, Academic Press, New York
Jost, P.C., Griffith, O.H., Capaldi, R.A. & Vanderkooi, G. (1973*a*) *Proc. Natl. Acad. Sci. U.S.A.* **70**, 480–484
Jost, P., Griffith, O.H., Capaldi, R.A. & Vanderkooi, G. (1973*b*) *Biochim. Biophys. Acta* **311**, 141–152
Jost, P.C., Capaldi, R.A., Vanderkooi, G. & Griffith, O.H. (1973*c*) *J. Supramol. Structure* **1**, 269–280
Jost, P.C., Nadakavukaren, K.K. & Griffith, O.H. (1977) *Biochemistry* **16**, 3110–3114
Kang, S.Y., Gutowsky, H.S., Hsung, J.C., Jacobs, R., King, T.E., Rice, D. & Oldfield, E. (1979*a*) *Biochemistry* **18**, 3257–3267
Kang, S.Y., Gutowsky, H.S. & Oldfield, E. (1979*b*) *Biochemistry* **18**, 3268–3271
Kang, S.Y., Rajan, S., Gutowsky, H.S., Kinsey, R. & Oldfield, E. (1981) *J. Biol. Chem.* **256**, 1155–1159
Kleeman, W. & McConnell, H.M. (1976) *Biochim. Biophys. Acta* **419**, 206–222
Kohler, S.J. & Klein, M.P. (1976) *Biochemistry* **15**, 967–973
Ladbrooke, B.D., Williams, R.M. & Chapman, D. (1968) *Biochim. Biophys. Acta* **150**, 333–340
Longmuir, K.J., Capaldi, R.A., & Dahlquist, F.W. (1977) *Biochemistry* **16**, 5746–5755
Marčelja, S. (1976) *Biochim. Biophys. Acta* **455**, 1–7
Marsh, D. Watts, A., Maschke, W. & Knowles, P.F. (1978) *Biochem. Biophys. Res. Commun.* **81**, 397–402
Moore, B.M., Lentz, B.R. & Meissner, G. (1978) *Biochemistry* **17**, 5248–5255
Neugebauer, D.-Ch., Blaurock, A.E. & Worcester, D.L. (1977) *FEBS Lett.* **78**, 31–35

O'Konski, C.T., Yoshioka, K. & Orttung, W.H. (1959) *J. Am. Chem. Soc.* **63**, 1558–1565
Oldfield, E. & Allerhand, A. (1975) *J. Biol. Chem.* **250**, 6403–6407
Oldfield, E. & Meadows, M. (1978) *J. Magn. Reson.* **31**, 327–335
Oldfield, E. & Rothgeb, T.M. (1980) *J. Am. Chem. Soc.* **102**, 3635–3637
Oldfield, E., Chapman, D. & Derbyshire, W. (1971) *FEBS Lett.* **16**, 102–104
Oldfield, E., Norton, R.S. & Allerhand, A. (1975*a*) *J. Biol. Chem.* **250**, 6368–6380
Oldfield, E., Norton, R.S. & Allerhand, A. (1975*b*) *J. Biol. Chem.* **250**, 6381–6402
Oldfield, E., Gilmore, R., Glaser, M., Gutowsky, H.S., Hshung, J.C., Kang, S.Y., King, T.E., **Meadows**, M. & Rice, D. (1978*a*) *Proc. Natl. Acad. Sci. U.S.A.* **75**, 4657–4660
Oldfield, E., Meadows, M. Rice, D. & Jacobs, R.(1978*b*) *Biochemistry* **17**, 2727–2740
Oster, O., Neireiter, G.W., Clouse, A.O. & Gurd, F.R.N. (1975) *J. Biol. Chem.* **250**, 7990–7996
Owicki, J.C., Springgate, M.W. & McConnell, H.M. (1978) *Proc. Natl. Acad. Sci. U.S.A.* **75**, 1616–1619
Papahadjopoulos, D., Moscarello, M., Eylar, E.H. & Isac, T. (1975)*Biochim. Biophys. Acta* **401**, 317–335
Rajan, S., Kang, S.Y., Gutowsky, H.S. & Oldfield, E. (1981) *J. Biol. Chem.* **256**, 1160–1166
Rice, D. & Oldfield, E. (1979) *Biochemistry* **18**, 3272–3279
Rice, D., Hsung, J.C., King, T.E. & Oldfield, E. (1979*a*) *Biochemistry* **18**, 5885–5892
Rice, D.M., Meadows, M.D., Scheinmann, A.O., Goni, F.M., Gomez, J.F., Moscarello, M.A., **Chapman**, D. & Oldfield, E. (1979*b*) *Biochemistry* **18**, 5893–5903
Rothgeb, T.M. & Oldfield, E. (1981) *J. Biol. Chem.* **256**, 1432–1446
Schlecht, P. (1969) *Biopolymers* **8**, 757–765
Schröder, H. (1977) *J. Chem. Phys.* **67**, 1617–1619
Scott, H.L. & Cherng, S.L. (1978) *Biochim. Biophys. Acta* **510**, 209–215
Siminovitch, D.J., Rance, M. & Jeffrey, K.R. (1980) *FEBS Lett.* **112**,79–82
Skarjune, R. & Oldfield, E. (1979) *Biochemistry* **18**, 5903–5909
Slichter, C.P. (1978) *Principles of Magnetic Resonance*, Springer-Verlag, New York
Stier, A. & Sackmann, E. (1973) *Biochim. Biophys. Acta* **311**, 400–408
Takano, T. (1977) *J. Mol. Biol.* **110**, 537–568
Wagner, G., DeMarco, A. & Wüthrich, K. (1976) *Biophys. Struct. Mech.* **2**, 139–158
Warren, G.B., Toon, P.A., Birdsall, N.J.M., Lee., A.G. & Metcalfe, J.C. (1974*a*) *Proc. Natl. Acad. Sci. U.S.A.* **71**, 622–626
Warren, G.B., Toon, P.A., Birdsall, N.J.M., Lee, A.G. & Metcalfe, J.C. (1974*b*) *Biochemistry* **13**, 5501–5507
Warren, G.B., Houslay, M.D., Metcalfe, J.C. & Birdsall, N.J.M. (1975) *Nature (London)* **255**, 684–687
Wooten, J.B. & Cohen, J.S. (1979) *Biochemistry* **18**, 4188–4191
Wüthrich, (1976) *N.m.r. in Biological Research: Peptides and Proteins*, American Elsevier, New York
Yeagle, P.L., Hutton, W.C., Huang, C. & Martin, R.B. (1975) *Proc. Natl. Acad. Sci. U.S.A.* **72**, 3477–3481